

RESEARCH ARTICLE

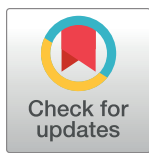
Characterization of the secretory profile and exosomes of limbal stem cells in the canine species

Antonio J. Villatoro^{1,2} , Cristina Alcoholado^{1,3,4} , María del Carmen Martín-Astorga¹, Gustavo Rico^{1,4,5}, Viviana Fernández², José Becerra^{1,4,5*}

1 Laboratory of Bioengineering and Tissue Regeneration (LABRET), Department of Cell Biology, Genetics and Physiology, Faculty of Sciences, University of Málaga, IBIMA, Málaga, Spain, **2** Instituto de Immunología Clínica y Terapia Celular (IMMUNESTEM), Málaga, Spain, **3** Biomedicine Research Institute of Malaga (IBIMA), Campus Universitario Teatinos, Málaga, Spain, **4** Networking Research Center on Bioengineering, Biomaterials and Nanomedicine, (CIBER-BBN), Malaga, Spain, **5** Andalusian Centre for Nanomedicine and Biotechnology-BIONAND, Málaga, Spain

 These authors contributed equally to this work.

* becerra@uma.es



OPEN ACCESS

Citation: Villatoro AJ, Alcoholado C, Martín-Astorga MdC, Rico G, Fernández V, Becerra J (2020) Characterization of the secretory profile and exosomes of limbal stem cells in the canine species. *PLoS ONE* 15(12): e0244327. <https://doi.org/10.1371/journal.pone.0244327>

Editor: Alexander V. Ljubimov, Cedars-Sinai Medical Center, UNITED STATES

Received: August 4, 2020

Accepted: December 7, 2020

Published: December 29, 2020

Copyright: © 2020 Villatoro et al. This is an open access article distributed under the terms of the [Creative Commons Attribution License](https://creativecommons.org/licenses/by/4.0/), which permits unrestricted use, distribution, and reproduction in any medium, provided the original author and source are credited.

Data Availability Statement: All relevant data are within the paper and its [Supporting Information](#) files.

Funding: GR was supported by the RD16/0011/0022 grant of the Spanish Network on Cell Therapy (TerCel). AV and VF were supported by the Contract Aljama Gestión SL-University of Malaga (8.06/5.02.5013). MM was supported by the UMA18-FEDERJA-133 grant of the Operational programme FEDER Andalucía 2014-2020. CA was supported by the Promotion of Youth Employment

Abstract

Limbal stem cells (LSCs) are a quiescent cell population responsible for the renewal of the corneal epithelium. Their deficiency is responsible for the conjunctivization of the cornea that is seen in different ocular pathologies, both in humans and in the canine species. The canine species represents an interesting preclinical animal model in ocular surface pathologies. However, the role of LSCs in physiological and pathological conditions in canine species is not well understood. Our objective was to characterize for the first time the soluble factors and the proteomic profile of the secretome and exosomes of canine LSCs (cLSCs). In addition, given the important role that fibroblasts play in the repair of the ocular surface, we evaluated the influence of the secretome and exosomes of cLSCs on their proliferation in vitro. Our results demonstrated a secretory profile of cLSCs with high concentrations of MCP-1, IL-8, VEGF-A, and IL-10, as well as significant production of exosomes. Regarding the proteomic profile, 646 total proteins in the secretome and 356 in exosomes were involved in different biological processes. Functionally, the cLSC secretome showed an inhibitory effect on the proliferation of fibroblasts in vitro, which the exosomes did not. These results open the door to new studies on the possible use of the cLSC secretome or some of its components to treat certain pathologies of the ocular surface in canine species.

Introduction

The cornea plays a fundamental role in clear vision. It has regeneration and repair capacity owing to the existence of a population of limbal stem cells (LSCs) residing within a cell niche in the transition zone between the cornea and the sclera (sclerocorneal limbus) in the so-called palisades of Vogt [1–3]. LSCs are a quiescent cell population with proliferative capacity that are responsible for the continuous renewal of the corneal epithelium, and their deficiency is responsible for corneal conjunctivization (vascularization, scarification, ulceration, chronic

and implementation of the Youth Guarantee in R&D&I, 2018 (PEJ2018-004785-A) grant of the Ministry of Science, Innovation and University. The funders had no role in study design, data collection and analysis, decision to publish, or preparation of the manuscript. VI National R&D&I Plan 2008–2011, Iniciativa Ingenio 2010, Consolider Program, CIBER Actions, Instituto de Salud Carlos III with assistance from the European Regional Development Fund and Regional Government of Andalusia (Junta de Andalusia, PAIDI (BIO217), provided support in the form of materials, but did not have any additional role in the study design, data Cover Letter collection and analysis, decision to publish, or preparation of the manuscript. There was no additional external funding received for this study.

Competing interests: The authors have declared that no competing interests exist.

inflammation, and loss of corneal transparency), which triggers corneal opacity and blindness [4–6].

The LSC niche is one of the most active stem cell niches preserved in adulthood, characteristic of tissues that need continuous regeneration. This niche, on a basal membrane, houses different cell populations, such as fibroblasts, melanocytes, immune cells, vascular endothelial cells, and mesenchymal stem cells (MSCs), among others [7, 8]. However, due to its cellular complexity and heterogeneity, there are still many unknowns about the roles of LSCs and their secretory and proteomic profiles. Previous studies suggest that in the LSC niche, different substances with biological activity responsible for the proper functioning of the niche are released [7].

Although LSCs have been studied in humans [9, 10], in recent years their role in physiological and pathological conditions in veterinary medicine has begun to be evaluated [11, 12]. Although LSC transplantation is a therapeutic strategy in human medicine in cases of damage or insufficiency [5, 13], whose purpose is to restore the integrity of the corneal epithelium, such therapy is nearly unknown in dogs [14]. To date, neither the secretory profile of canine LSCs (cLSCs) nor their exosomes have been characterized. There are no studies on the interaction of cLSCs with other cell types located in its niche that play an important role in certain ocular pathologies. In this context, the formation of scar on the corneal surface is a frequent complication of corneal stromal healing in response to surgery, trauma, or infection, disturbing visual clarity. The cells responsible for the formation of scars are mitotically active fibroblasts originating from stromal keratocytes [15]. There is little literature on the role of LSCs in stromal healing [16].

The objectives of this study were (1) to characterize for the first time the soluble components and the proteomic profile of the cLSC secretome under standard culture conditions; and (2) to isolate, characterize, and determine the proteomic profile of the cLSC exosomes and compare these with those of the secretome. Finally, given the important role that fibroblasts play in the corneal stroma and in the sclerocorneal niche, we studied the *in vitro* effects of the secretome and exosomes of cLSCs.

Materials and methods

All procedures with animals were performed by veterinarians in compliance with national and European legislation (Royal Decree RD1201/2005 and Directive 86/609/EEC of the EU, modified by 2003/65/EC, respectively) for the protection of animals used for research experimentation and other scientific purposes. Likewise, the protocols were approved by the Institutional Committee for the Care and Use of Animals of BIONAND (Andalusian Center for Nanomedicine and Biotechnology), Malaga, Spain, and written consent was obtained from all dog owners.

Isolation, expansion and proliferation of cLSCs

Intact eyes of four young dogs free of any ocular pathology were extracted immediately after their slaughter, which was performed for reasons unrelated to this study. The eyes were immersed in Dulbecco's modified Eagle medium (DMEM) supplemented with 2.5 mM L-glutamine, 100 U/ml penicillin, 100 µg/mL streptomycin, and 1.25 µg/mL fungizone (Merck) and transported to our laboratory at 4°C, where they were processed within two hours postextraction.

On a sterile glass Petri dish, each eye was washed with saline, and with the aid of scalpel, scissors, and sterile forceps, fragments of approximately 0.5 x 0.5 cm of limbo-corneal tissue were obtained. After removal of iris debris and excess sclera, each explant was positioned with the epithelial surface upward in six-well plates with 3 ml of medium supplemented with 10% fetal bovine serum (FBS). This supplemented medium was composed of Dulbecco's modified

Eagle medium (DMEM), 10% FBS, 2.5 mM L-glutamine, 100 U/ml penicillin, 100 µg/mL streptomycin, and 1.25 µg/mL fungizone (Merck) and will be referred to as supplemented medium.

The plates were incubated for three days under standard conditions (37°C, 95% humidity and 5% CO₂), allowing cell migration from the explant to the wells. Then the explants were removed, each well was washed with 1 ml of phosphate-buffered saline (PBS), and 3 ml of supplemented medium was added to allow cell proliferation. Medium was refreshed every three days until the cells reached a confluence of 80%, at which time the subculture was performed. To do this, 0.5 ml of trypsin (Merck) was used per well, and the cells obtained were seeded in FT-75 flasks at a density of 8x10⁵ cells per bottle. Each donor was cultured individually and later frozen in 90% FBS and 10% dimethylsulfoxide (DMSO, Merck). All experiments were performed in cells of culture passage 2.

For the cLSC proliferation assay, we used the MTS colorimetric method (CellTiter 96 Aqueous One Solution Cell Proliferation Assay, Promega) following previously published protocols [17, 18]. For this, we plated 3000 cells/well in a 96-well plate with medium supplemented with 10% FBS. Medium was refreshed every two days, and readings were taken with a spectrophotometer (ELx800, Bio-Tek instruments) at a wavelength of 490 nm on days 1, 3, 6, 8, 10, and 13.

Characterization of cLSCs

Using Western blot (WB), the expression of typical LSC markers ATP-binding cassette superfamily G member 2 (ABCG2), p63, anti-p40-deltaNp63, and vimentin was measured as described in the literature [4, 11, 12]. First, cellular proteins from cLSCs were extracted using RIPA buffer with protease inhibitors. This extract was kept on ice for 30 minutes, and the lysis mixture was centrifuged at 11,000 g and 4°C for 15 minutes. The supernatant was transferred to a new tube, and the protein concentration was determined using the bicinchoninic acid kit (BCA, SERVA).

For WB, 30 µg of protein was used, and the membranes were incubated with mouse anti-ABCG2 (Abcam, ab108312), mouse anti-p63 (Abcam, ab124762), anti-vimentin (Santa Cruz Biotechnology, sc-6260) and rabbit anti-deltaNp63 (Abcam, ab203826) at 1:1000 dilution. As a positive control for ABCG2, p63 and deltaNp63, a protein lysate from the HeLa cell line (Merck) was used, and in the case of vimentin, a protein lysate of human MSC from adipose tissue (hAd-MSC) was used as a positive control. Secondary anti-mouse (Merck) and anti-rabbit (Abcam) antibodies were used for detection by ECL (SERVA), and the results were visualized in the ChemiDoc™ XRS + system (Bio-Rad).

Obtaining the cLSC secretome

To obtain the cLSC secretome, 1.5 x 10⁶ cLSCs were seeded into FT-175 flasks with supplemented medium. Medium was refreshed twice a week. Once 80% confluence was reached, the medium was removed, and 20 ml supplemented medium per bottle was added. The cultures were maintained for 72 hours in the incubator, after which their conditioned medium was removed, passed through a 0.22-µm filter to remove cell debris, and frozen at -20°C. The cells of each flask were detached with trypsin and counted in a Neubauer chamber, and their viability was evaluated with trypan blue staining.

cLSC secretory profile

For the quantification of cytokines and growth factors present in the cLSC secretome, an equal mixture of the media from the different donors was used. A commercial canine cytokine

11-plex assay (Thermo Fisher Scientific) was used, with which the concentration of 11 analytes was determined by Luminex technology: one chemokine (monocyte chemoattractant protein-1, MCP-1), cytokines (interleukin (IL)-2, IL-6, IL-8, IL-10, IL-12p40, tumor necrosis factor- α , interferon- γ), and growth factors (nerve growth factor- β , stem cell factor, vascular endothelial growth factor (VEGF)-A) [19]. The amounts obtained were normalized and are expressed in picograms per milliliter per million cells.

Isolation and characterization of exosomes

To obtain the exosomes, 1×10^6 cLSCs were seeded in each FT-175 flask with supplemented medium. Upon reaching 80% confluence, the flasks were washed with PBS, and medium supplemented with 10% FBS free of exosomes (ensured by prior ultracentrifugation at 100,000 g for 60 minutes at 4°C) was added. The medium was removed after 72 hours of incubation, the cells were counted in a Neubauer chamber, and their viability was evaluated with trypan blue.

The exosomes were isolated by ultracentrifugation as we have previously described [19]. In brief, the samples were centrifuged at 13,000 g and 4°C for 30 minutes to remove cell debris and microvesicles. Next, they were ultracentrifuged twice at 100,000 g for 60 minutes and 4°C using the ^{70}Ti fixed-angle rotor in an Optima LE-80K ultracentrifuge (Beckman Coulter). The precipitate (exosomes) was resuspended in 100 μL of PBS to obtain a homogeneous solution. The exosomes were quantified using the BCA kit (Thermo Scientific) and stored at -20°C until use. Each sample was processed individually, and an equal mixture of each donor was performed to characterize the exosomes.

Transmission electron microscopy. A sample of 20 μL exosomes from cLSCs was resuspended in 0.1 M HEPES solution (pH 7.4) (Merck), and a drop was placed on a carbon-coated nickel grid (Aname) and allowed to dry overnight. Images of the samples were taken at different magnifications in a transmission electron microscope (TEM).

Determination of the size distribution and electronegativity. The exosomes were resuspended in 1 ml of PBS, and the size distribution and Z potential (electronegativity) were analyzed at 25°C using a Zetasizer Nano ZS (Malvern Instruments).

Western blot. The exosomes of cLSCs were characterized by WB for specific markers [20]. Briefly, 30 μg of exosomal proteins were used, and the membranes were incubated overnight with rabbit anti-ALIX (Abcam, ab186429), anti-TSG101 (Abcam, ab125011) and anti-calnexin (Cell Signaling Technology, 2679) antibodies at 1:1000 dilution. A protein lysate from human MSC from adipose tissue (hAd-MSC) was used as a positive control. Secondary anti-rabbit antibody (Abcam, ab6721) was used for detection by ECL (SERVA), and the results were visualized in the ChemiDoc XRS + system (Bio-Rad).

Proteomic analysis of the secretome and exosomes of cLSCs

In the production of the secretome for proteomic analysis, the standard culture medium was replaced by DMEM without supplementation when the cell culture had reached 80% confluence. After 24 hours of incubation under standard conditions, the secretome was removed, filtered through a 0.22- μm , and frozen at -80°C. This secretome was lyophilized in the LyoQuest lyophilizer (TELSTAR) and reconstituted in a volume of 500 μL .

The proteomic profile was determined on an equal mixture of secretomes from different donors in the Proteomics Service of the SCAI of the University of Malaga, as described previously [19]. The tandem mass spectrometry data were compared against the SwissProt and NCBI nr databases according to the parameters described for “biological process” provided by the Gene Ontology resource.

Activity of the secretomes and exosomes of cLSCs on fibroblasts

MTS proliferation assay. For the proliferation assay, 3000 canine fibroblasts (directly obtained from Cellider Biotech, catalogue number CFB001F) were seeded per well in a 96-well plate with the following conditions: control (100 μ L medium supplemented with 10% FBS/well), secretome generated under standard conditions as described in section 3.3 (100 μ L/well), and cLSC exosomes (25 μ g/ml per well, added on days 1 and 5). The medium was refreshed every two days, and the proliferation was measured on days 1, 2, 5, 7, and 9 in the spectrophotometer (ELx800, Bio-Tek instruments) using the MTS assay (CellTiter 96 Aqueous One Solution Cell Proliferation Assay, Promega).

Wound-healing assay on canine fibroblasts in response to the cLSC secretome. Based on the results obtained above in the MTS assay, we evaluated the proliferation/migration capacity of fibroblasts using the wound healing assay. For this, canine fibroblasts were seeded at a density of 50,000 cells/cm² in 24-well plates and kept in supplemented medium for 48 hours until they reached confluence. Using a pipette tip, a wound was generated in a straight line in the center of the well. Then, 500 μ L of supplemented medium (C-) and the secretome from cLSCs (n = 4) were added.

The cultures were photographed with digital phase-contrast technology in an automated manner using an *Operetta High Content Screening* (HCS) system (Perkin Elmer) 0, 3, 7, 24, 48, and 120 hours after the application of the treatment.

The size of the open areas (areas without cells, corresponding to the scratch) was calculated by processing and analyzing the images with ImageJ software, applying the MRI *wound healing tool* (http://dev.mri.cnrs.fr/projects/imagejmacros/wiki/Wound_Healing_Tool). The open areas corresponding to time 0 were considered as 100%, and the rest of the areas were compared to this value for each replicate separately. Additionally, the shrinkage rate of the wound area was calculated for the period between 0 and 48 hours by calculating the slope in terms of mm²/day (Fig 6B). The average \pm SD of each condition is shown (n = 4).

Statistical analysis

Statistical analysis for the MTS proliferation assay was performed using one-way analysis of variance (ANOVA). In the case of the wound healing assay, the analysis used was two-way ANOVA for repeated measurements. Multiple comparisons between the different conditions were performed by a post hoc analysis using the Holm-Sidak method.

Results

Isolation and expansion of cLSCs

The cLSCs began to migrate from the explant after 3 days of incubation, showing the characteristic morphology of this cell type (Fig 1A) and a proliferation that we could observe in the growth curve over 13 days at a culture passage 2 (Fig 1B).

Western blot of the protein lysates of the cLSCs

Positive expression of the specific markers ABCG2, p63, anti-p40-deltaNp63, and vimentin in cLSCs was observed by WB in the protein lysates of these cells (Fig 1C).

Characterization of the secretome composition by immunoassay

When the concentrations of the 11 analytes evaluated were quantified, we found higher amounts of MCP-1, IL-8, VEGF-A, and IL-10. The values obtained were normalized per million cells (Fig 2).

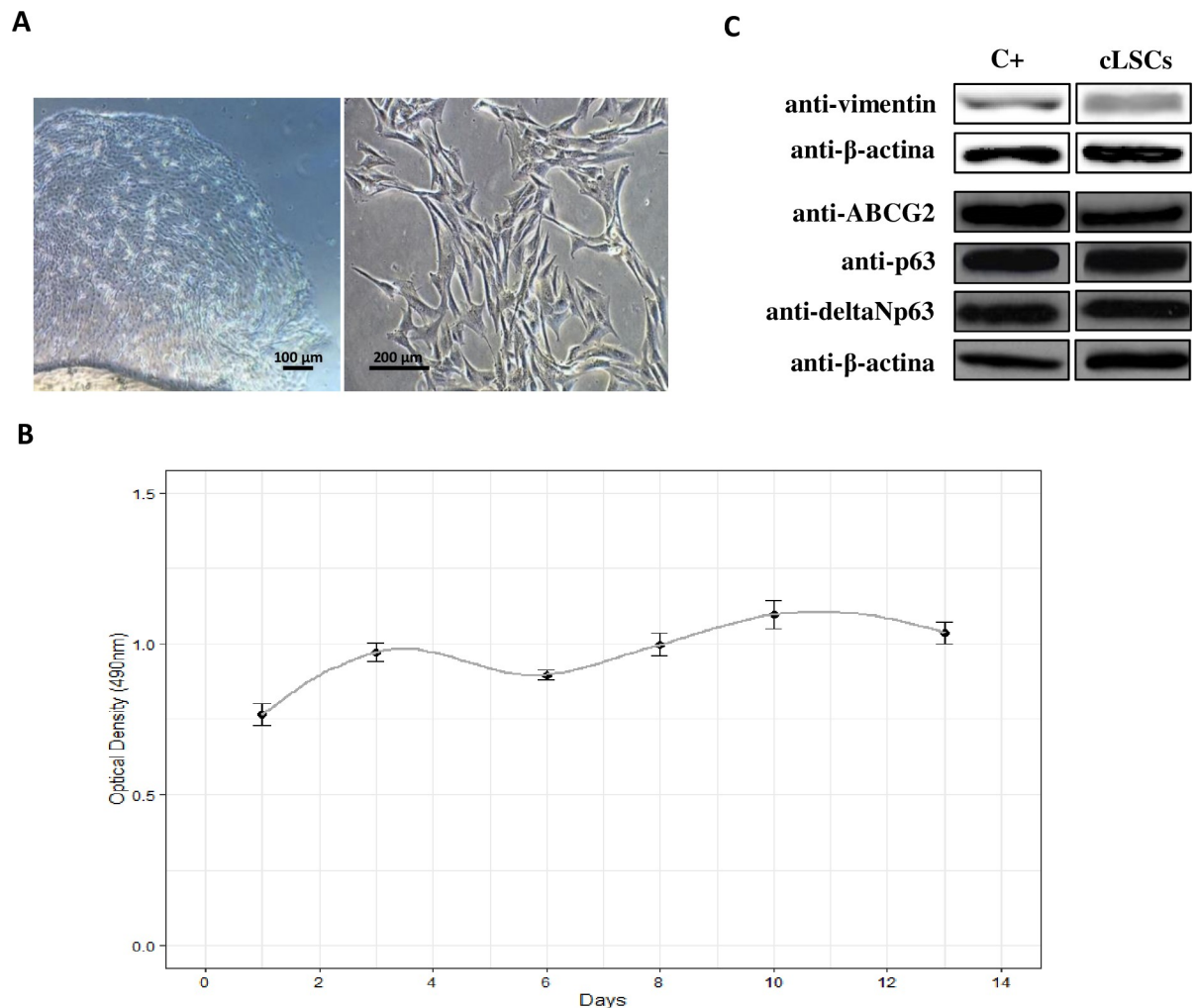


Fig 1. Isolation and characterization of cLSC. (A) Images were taken in culture passage 0 and 1, at 4x and 20x magnification respectively, under a bright field microscope. (B) Growth curve of cLSCs at culture passage 2 for 13 days by MTS assay. (C) Expression of ABCG2, p63, anti-p40-deltaNp63, and vimentin markers by WB. Positive control for ABCG2, p63 and deltaNp63 is a protein lysate from HeLa cell line; positive control for vimentin is a protein lysate of hAd-MS.

<https://doi.org/10.1371/journal.pone.0244327.g001>

Characterization of the exosomes of limb cells

The exosomes of cLSCs examined by TEM showed a diameter less than 50 nm (Fig 3A). This was confirmed by dynamic light scattering to observe the size range of the isolated exosomes (Fig 3B). The detected Z potential was -11.8 ± 1.15 mV, and the polydispersity index (0.42) was indicative of a homogeneous sample. Fig 3C shows the positive expression of specific exosomal markers, such as ALIX and tumor susceptibility gene 101 (TSG101), and negative expression for calnexin.

Proteomic analysis of the secretome and exosomes

The numbers of total proteins present in the secretome and exosomes of cLSCs were determined by mass spectrometry. For the bioinformatic analysis, the peptide database of the species *Canis lupus familiaris* was used. There were a total of 646 proteins in the secretome (light gray) and 356 in the exosomes (dark gray), and 218 proteins were shared in common between the secretome and exosomes (Fig 4A). These proteins were grouped according to the GO

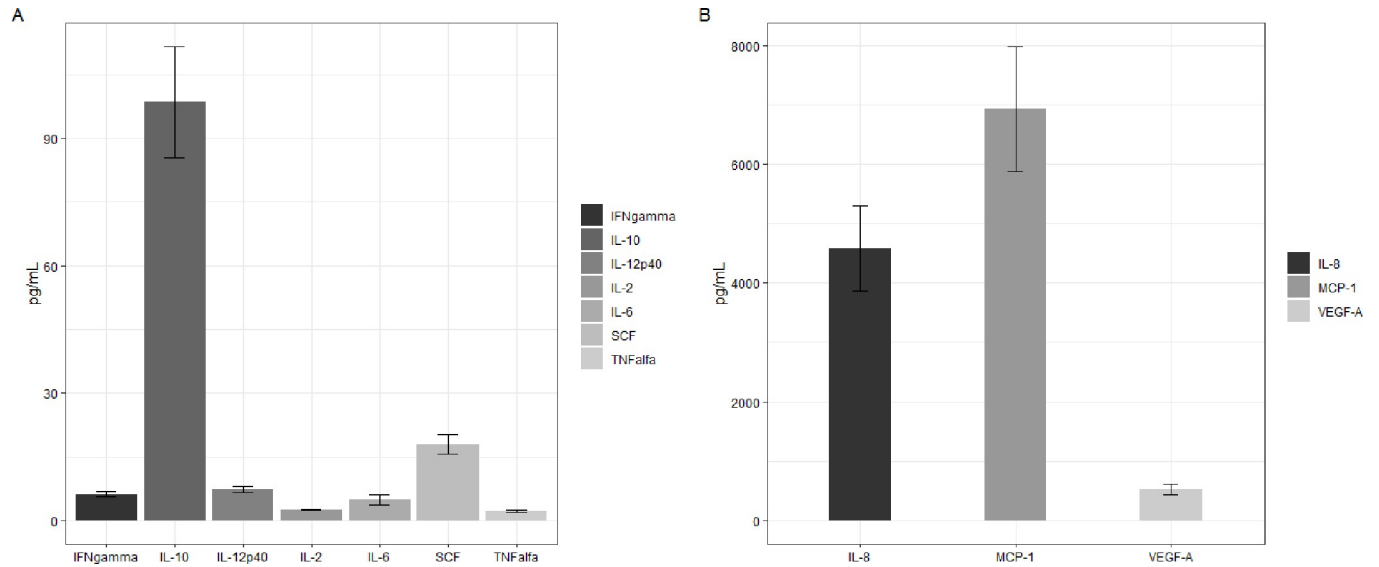


Fig 2. Profile of cytokines and growth factors present in cLSC secretome. (A) Analytes found in lower concentration. (B) Analytes more abundant in the secretome. Analyte concentrations are expressed as picograms/ml per million cells.

<https://doi.org/10.1371/journal.pone.0244327.g002>

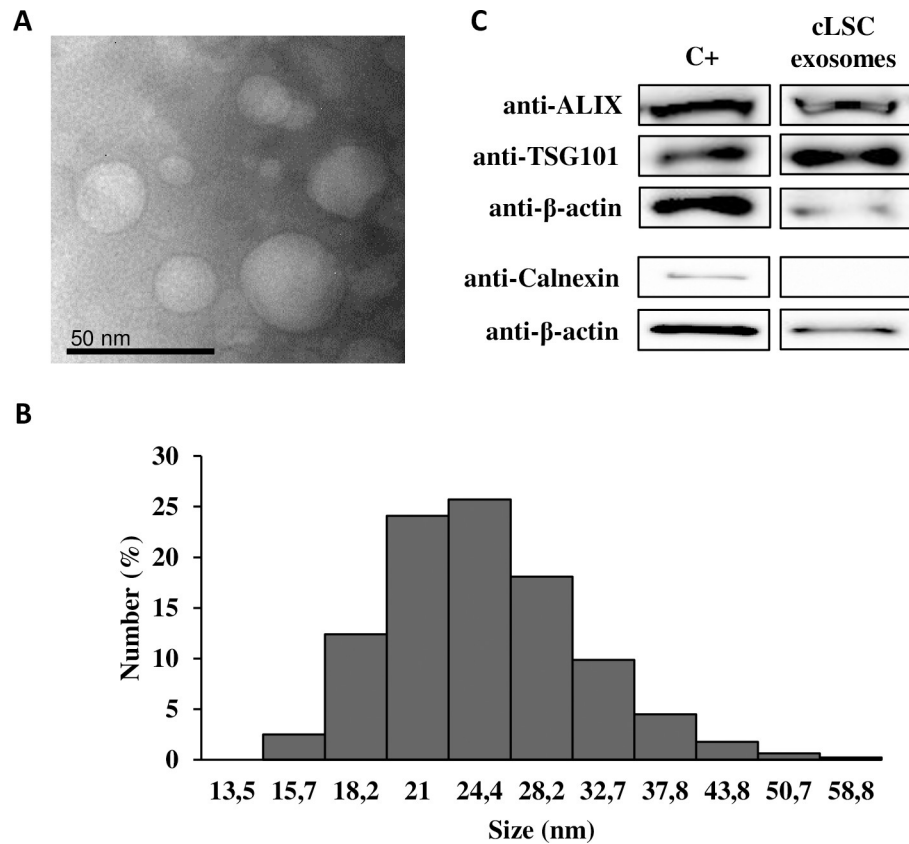


Fig 3. Exosome characterization. (A) Representative images of TEM. (B) Size distribution of exosomes using Zetasizer. (C) WB analysis of specific exosomal markers. A protein lysate of hAd-MSC was taken as positive control.

<https://doi.org/10.1371/journal.pone.0244327.g003>

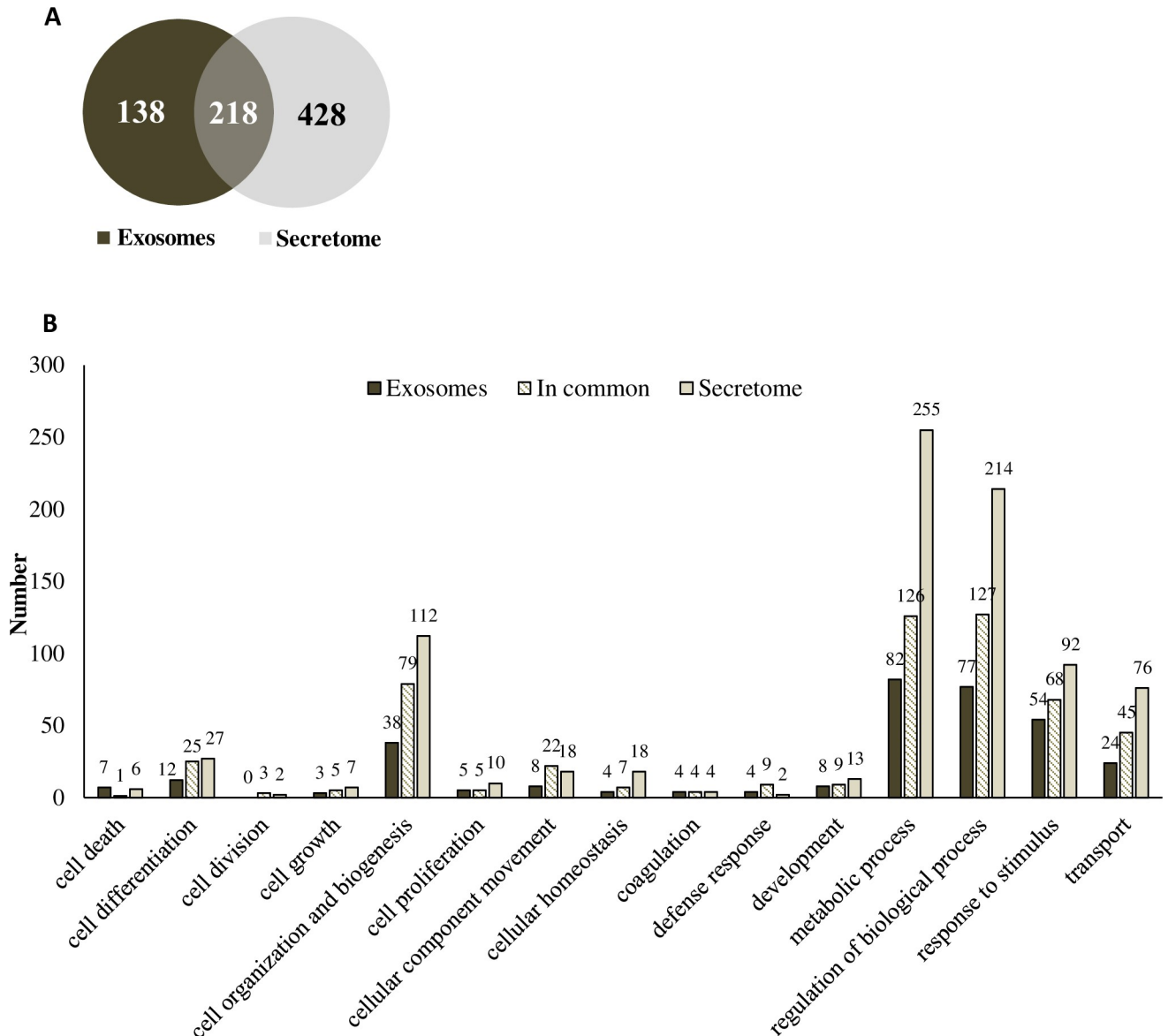


Fig 4. Proteomic analysis of cLSC secretome and exosomes. (A) Venn diagram showing the proteins present in exosomes (dark grey), secretome (light grey) and those common to both samples (overlapping colours). (B) Comparison of the biological processes involving the characterized proteins for exosomes (dark grey), secretome (light grey) and in common (striped) of cLSC according to Gene Ontology parameters.

<https://doi.org/10.1371/journal.pone.0244327.g004>

“biological processes” they are involved in according (Fig 4B). A specific list of all proteins material is indicated in the S1 and S2 Tables.

Proliferation assays of canine fibroblasts under the influence of the limbal secretome

The cLSC secretome showed inhibitory activity on the proliferation of canine fibroblasts, stopping this proliferation for the 9 days of the MTS assay (Fig 5). However, the exosomes of cLSCs did not show statistically significant differences from the control. It follows that the observed activity should be concentrated in the soluble fraction of the cLSC secretome and not in their exosomes.

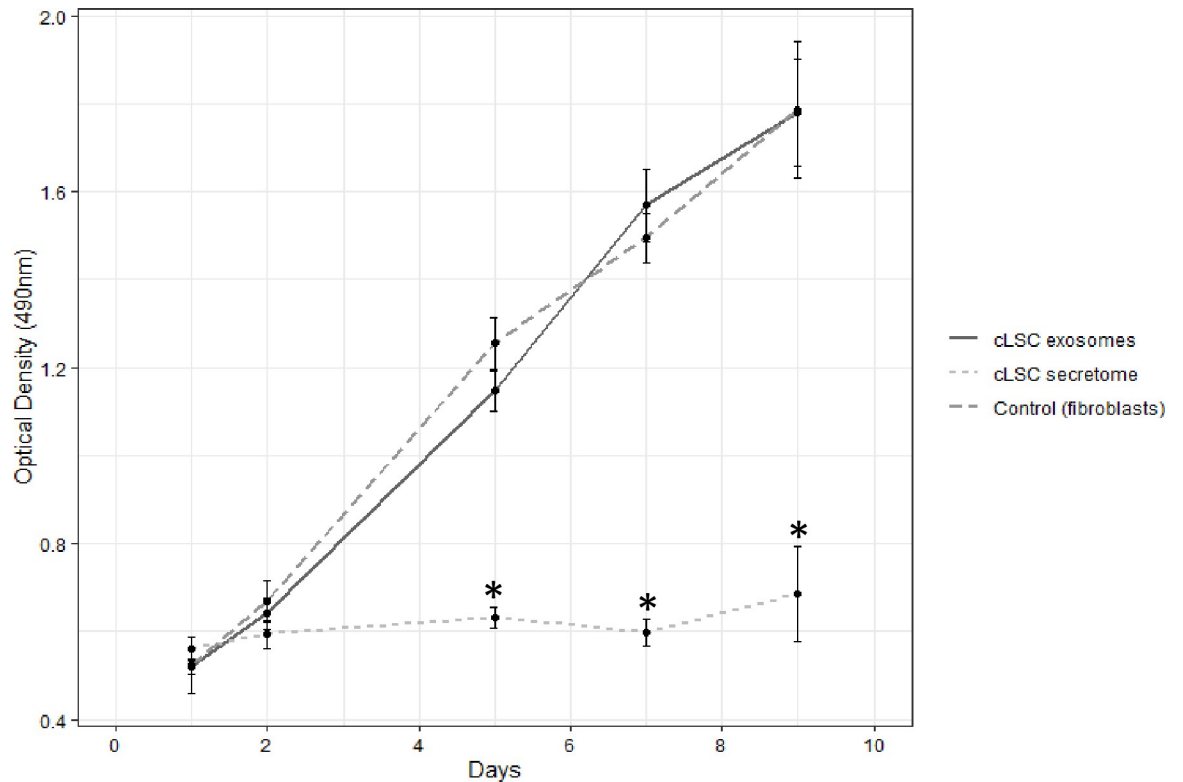


Fig 5. Proliferation assay. MTS showing the influence of exosomes (continuous dark grey curve) and secretome (discontinuous light grey curve) of cLSC on fibroblasts in culture (discontinuous dark grey curve). Statistically significant differences are shown on days 5, 7 and 9 * $p < 0.001$ of the secretome versus exosomes and control condition.

<https://doi.org/10.1371/journal.pone.0244327.g005>

Scratch-wound assay. Fig 6 shows the effect of cLSC secretome treatment compared to the control medium on the migration of canine fibroblasts. At 48 hours posttreatment, the closure rate of the fibroblasts treated with control medium was $1.88 \text{ mm}^2/\text{day}$, while treatment with the cLSC secretome significantly decreased the migration/growth rate to $1.36 \text{ mm}^2/\text{day}$ ($p < 0.001$) (Fig 6B).

In the analysis of the percentage of open area, after 24 hours these areas were 4% higher in cultures treated with the secretome than in negative controls. This effect was statistically significant after 48 hours of treatment (Fig 6C). Fibroblasts treated with control medium migrated to decrease the open area to 5.07% of the initial area, while in cultures treated with the secretome, this area still made up on average 16.15%.

Discussion

The regenerative processes of the cornea are complex mechanisms essential to ensure corneal transparency and visual function [16]. In this process, LSCs are responsible for the maintenance of the corneal epithelium through centripetal migration from their niche and their subsequent differentiation into corneal epithelial cells [21].

In the niche where they dwell, there are other cell types whose homeostasis depends on their interrelation [7, 22]. Within this specialized microenvironment, a great variety of signals are triggered through precise cellular and molecular mechanisms, which are just beginning to be elucidated [23], but knowledge of these signals is fundamental to understanding the processes of corneal repair/regeneration and to opening possibilities to new biological therapeutic strategies.

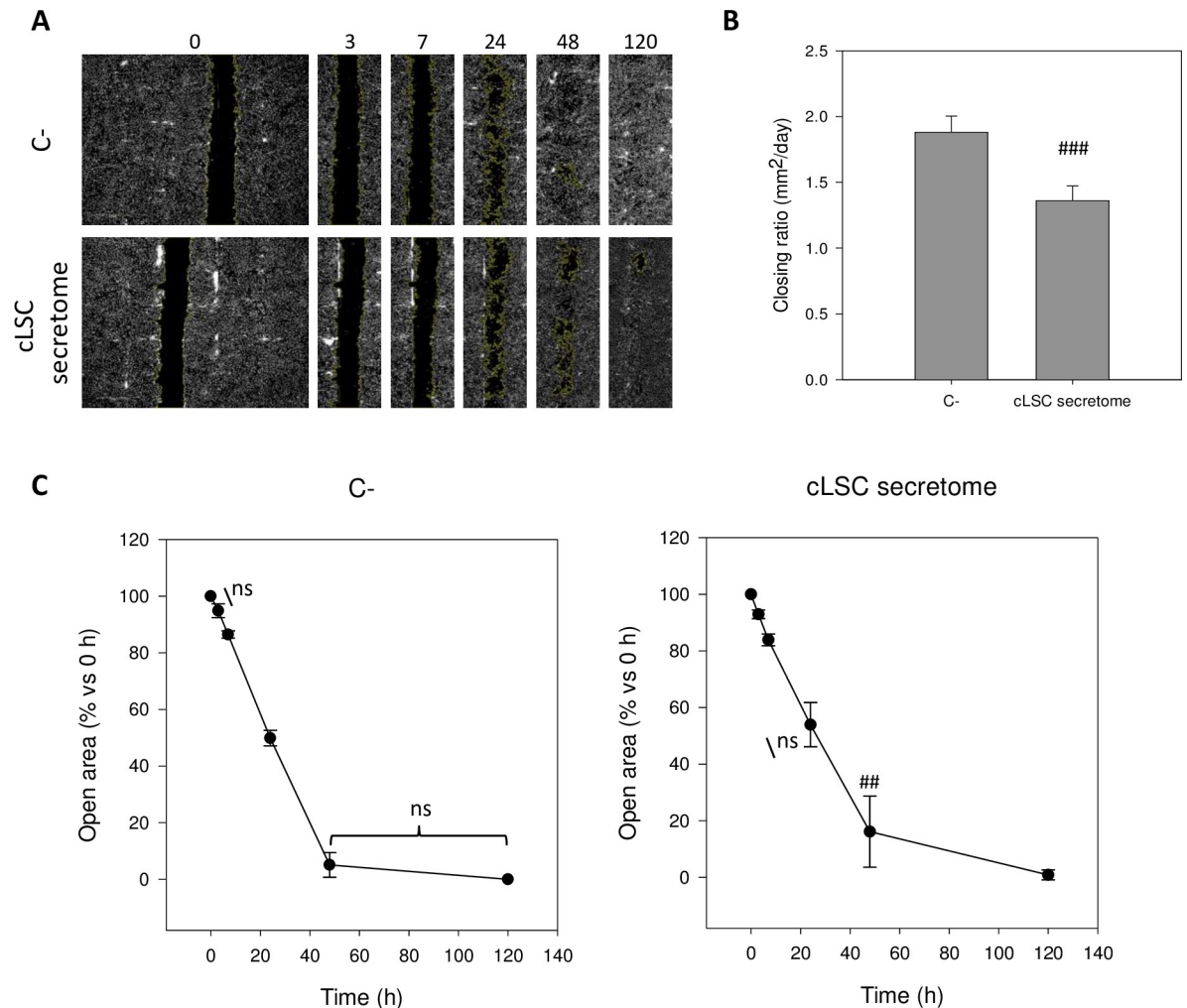


Fig 6. "Wound healing" test. (A) Example of representative replica photographs for each treatment and automatic detection of open areas. (B) Average rate of wound closure (in mm²/day) between 0 and 48h after treatment. (C) Evolution of the average open areas in time after the generation of the wound and the application of the treatment with control medium (C-) or cLSC secretome. Significant differences were detected between each time and the time immediately after, except for those indicated as not significant (ns). ##*p*<0.01; ###*p*<0.001; indicate significant differences between the marked condition and its C- homologous condition.

<https://doi.org/10.1371/journal.pone.0244327.g006>

In this study, cLSCs were isolated from the sclerocorneal limbus by explant, and we proceeded to expand them in the laboratory without losing their undifferentiated nature. The cultures expressed markers such as ABCG2, p63, anti-p40-deltaNp63 and vimentin, related to typical characteristics of LSCs in different species [3, 24], including the canine species [12], confirming their origin from the basal limbal epithelium [25].

This study is the first to characterize soluble factors and the proteomic profile of the secretome and exosomes of cLSCs in culture. When analyzing their secretory profile, we quantified 11 soluble factors with different biological activities. Among them, MCP-1, IL-8, and VEGF were the most highly expressed, and IL-10 was also high. MCP-1, also known as CCL2, is a proinflammatory chemokine involved in the recruitment or migration of different cell types of the immune system and plays a direct mediating role in angiogenesis [26]. IL-8 or CXCL8 is a chemokine with the ability to induce chemotaxis and neutrophil degranulation, contributing to the elimination of pathogens, and it has a potent angiogenic capacity that promotes venous

endothelial proliferation [27]. Through both of these cytokines, cLSCs could play important roles in inflammation and defense of the corneal surface against pathogens. When a pathogen comes into contact with the ocular surface, the innate immune system is activated, inducing a complex cascade of events, including the upregulation of proinflammatory cytokines involved in the repair of the ocular surface [28, 29].

VEGF is a signaling protein involved in the vasculogenesis and angiogenesis, in addition to manifesting vasodilator effects and increasing vascular permeability [30]. Through these actions, it plays an important role in the maintenance and nutrition of the abundant vascular structures of the sclerocorneal limbus [7, 31].

IL-10 is a pleiotropic cytokine with anti-inflammatory effects related to the induction of immune tolerance [32] and can intervene in the immune privilege enjoyed by the ocular surface. The ocular immune privilege confers immunological protection against the inflammatory response to organs, minimizing the risk of vision loss through strategies that modulate the innate and adaptive immune response and increase the immunological tolerance to different antigens [33, 34].

The proteomic profile of the cLSC secretome showed the existence of 646 different proteins, mainly assigned to functions such as transport, metabolism, regulation of different biological functions, cell differentiation, biogenesis, and response to stimuli.

Like other canine cell types [19], cLSCs produce exosomes, as shown by the characteristics that have been established for their identification, complying with the recommendation of the International Society of Extracellular Vesicles [20]. Exosomes are extracellular vesicles formed by a membrane unit that carries cargo that contains different bioactive molecules. They exert their effects by fusion with the target cells and transferring their cargo, playing a fundamental role in the intercommunication between the cells [35, 36]. Its role in corneal repair has been recently described in studies that evaluated exosomes of different cell types [37–39]. Through proteomic analysis of exosomes, we identified 356 proteins, mainly related to functions such as the regulation of different biological processes, metabolism, and response to stimuli. In addition, 218 proteins were shared between the proteomic profiles of the secretome and exosomes of cLSCs, among which we found proteins related to angiogenesis, growth, inflammation, metabolism, and cell signaling (S1 and S2 Tables).

The cargo of exosomes is specific to their cellular origin, but within the same species, a group of proteins essential for vesicular biogenesis, structure, and distribution is shared between exosomes from different cell types [35, 36]. To date, there is no specific description of common exosomal proteins of different origins in canine species. For this reason, when comparing cLSC proteomes with those of bone marrow and adipose tissue MSC exosomes previously published by our group [19], we discovered that they share nine proteins that have common functions related to biogenesis and cellular organization, regulation of biological processes, cellular metabolism, and transport (S1 and S2 Tables).

One of the most serious complications of corneal surface healing is the formation of eschar, whose persistence significantly compromises the transparency of the cornea [16, 40]. During its healing, the keratocytes of the corneal stroma differentiate into fibroblasts and myofibroblasts to induce the accumulation of extracellular matrix. This matrix is composed of altered glycosaminoglycans that contribute to reducing the transparency of scar tissue [41–43]. Although there is very little information on the role of LSCs in corneal stromal healing and their possible interaction with fibroblasts, we demonstrated *in vitro* that cLSCs were capable of inhibiting the proliferation and migration of fibroblasts. This inhibition occurred through the soluble factors of the secretome, as the application of their exosomes did not have an effect on proliferation or migration.

Considering all this, we conclude that LSCs, in the heterocellular complexity of the sclero-corneal niche, maintain a delicate balance in the regeneration of the ocular surface [39, 44]. LSCs in homeostatic conditions maintain a quiescent state [45] and play a central role in the maintenance of the niche through different molecules of their secretome, maintaining the vascular balance of the sclerocorneal limbus, defending against pathogens, and contributing to ocular immune privilege, in addition to exerting an inhibitory effect on the proliferation of corneal fibroblasts.

Recently, MSCs have been isolated and identified from the central and limbal stroma of the cornea in dogs [46], which opens new possibilities for future studies of the interconnection between both cell types to determine the contributions of cLSCs and MSCs in sclero-corneal physiological conditions and in ocular pathologies in canine species. LSC deficiency leads to corneal conjunctivization, whose progression leads to blindness [6]. This pathology has also been related to immune-mediated eye diseases of domestic species such as keratoconjunctivitis sicca and canine chronic superficial keratitis, as well as eosinophilic keratitis in cats and horses [2]. Our group has been a pioneer in describing the safety and efficacy of treatment with MSCs in both canine keratoconjunctivitis sicca [18] and feline eosinophilic keratitis [17]. We believe that the data provided in this study warrant new studies on the possible implantation of cLSCs alone or associated with MSCs in the treatment of such canine ocular pathologies.

Our study has certain limitations, such as the small number of donors, lack of specific markers, and a limited database of proteome studies for canine species.

All of the above leads us to propose that future objectives should focus on understanding the differentiation of LSCs during the regeneration/repair of the cornea and their relationship with other cell populations in order to better understand corneal pathophysiology. This knowledge will help to select the specific areas of the limbus or other parts of the cornea for the establishment of a cLSC culture for therapeutic purposes or as producers of secretomes and exosomes *in vitro*, which could be prepared in different pharmaceutical preparations and could be used as therapeutic elements.

Supporting information

S1 Table. Specific listing of cLSC exosome and secretome proteins according to the biological processes of GO.

(PDF)

S2 Table. Comparison of cLSC exosome proteins with bone marrow and adipose tissue MSC exosome proteins according to the biological processes of GO.

(PDF)

S1 Raw images.

(PDF)

Author Contributions

Conceptualization: Antonio J. Villatoro, Cristina Alcoholado, Gustavo Rico, Viviana Fernández, José Becerra.

Data curation: Cristina Alcoholado.

Formal analysis: Antonio J. Villatoro, Cristina Alcoholado, María del Carmen Martín-Astorga, Gustavo Rico.

Funding acquisition: José Becerra.

Investigation: Antonio J. Villatoro, Cristina Alcoholado, María del Carmen Martín-Astorga, Gustavo Rico, Viviana Fernández, José Becerra.

Methodology: Cristina Alcoholado, María del Carmen Martín-Astorga, Gustavo Rico.

Project administration: José Becerra.

Resources: José Becerra.

Software: Cristina Alcoholado, Gustavo Rico.

Supervision: Antonio J. Villatoro, José Becerra.

Validation: Antonio J. Villatoro, José Becerra.

Visualization: Antonio J. Villatoro, Cristina Alcoholado, José Becerra.

Writing – original draft: Antonio J. Villatoro, Cristina Alcoholado.

Writing – review & editing: Antonio J. Villatoro, Cristina Alcoholado, María del Carmen Martín-Astorga, Gustavo Rico, Viviana Fernández, José Becerra.

References

1. Goldberg MF, Bron AJ. Limbal palisades of Vogt. *Trans Am Ophthalmol Soc* 1982; 80:155–71. PMID: [7182957](#)
2. Sanchez RF, Daniels JT. Mini-Review: Limbal Stem Cells Deficiency in Companion Animals: Time to Give Something Back? *Curr Eye Res* 2016; 41(4):425–32. <https://doi.org/10.3109/02713683.2015.1056801> PMID: [26287764](#)
3. Notara M, Schrader S, Daniels JT. The porcine limbal epithelial stem cell niche as a new model for the study of transplanted tissue-engineered human limbal epithelial cells. *Tissue Eng Part A* 2011; 17(5–6):741–50. <https://doi.org/10.1089/ten.TEA.2010.0343> PMID: [20929285](#)
4. Patruno M, Perazzi A, Martinello T, Blaseotto A, Di Iorio E, Iacopetti I. Morphological description of limbal epithelium: searching for stem cells crypts in the dog, cat, pig, cow, sheep and horse. *Vet Res Commun* 2017; 41(2):169–173. <https://doi.org/10.1007/s11259-017-9676-y> PMID: [28110374](#)
5. Gonzalez G, Sasamoto Y, Ksander BR, Frank MH, Frank NY. Limbal stem cells: identity, developmental origin, and therapeutic potential. *Wiley Interdiscip Rev Dev Biol* 2018; 7(2).
6. Dua HS, Saini JS, Azuara-Blanco A, Gupta P. Limbal stem cell deficiency: concept, aetiology, clinical presentation, diagnosis and management. *Indian J Ophthalmol* 2000; 48(2):83–92. PMID: [11116520](#)
7. Li W, Hayashida Y, Chen YT, Tseng SC. Niche regulation of corneal epithelial stem cells at the limbus. *Cell Res* 2007; 17(1):26–36. <https://doi.org/10.1038/sj.cr.7310137> PMID: [17211449](#)
8. Funderburgh JL, Funderburgh ML, Du Y. Stem Cells in the Limbal Stroma. *Ocul Surf* 2016; 14(2):113–20. <https://doi.org/10.1016/j.jtos.2015.12.006> PMID: [26804252](#)
9. Ahmad S, Osei-Bempong C, Dana R, Jurkunas U. The culture and transplantation of human limbal stem cells. *J Cell Physiol* 2010; 225(1):15–9. <https://doi.org/10.1002/jcp.22251> PMID: [20506173](#)
10. Li GG, Zhu YT, Xie HT, Chen SY, Tseng SC. Mesenchymal stem cells derived from human limbal niche cells. *Invest Ophthalmol Vis Sci* 2012; 53(9):5686–97. <https://doi.org/10.1167/iops.12-10300> PMID: [22836771](#)
11. Morita M, Fujita N, Takahashi A, Nam ER, Yui S, Chung CS, et al. Evaluation of ABCG2 and p63 expression in canine cornea and cultivated corneal epithelial cells. *Vet Ophthalmol* 2015; 18(1):59–68. <https://doi.org/10.1111/vop.12147> PMID: [24471763](#)
12. Nam E, Fujita N, Morita M, Tsuzuki K, Lin HY, Chung CS, et al. Comparison of the canine corneal epithelial cell sheets cultivated from limbal stem cells on canine amniotic membrane, atelocollagen gel, and temperature-responsive culture dish. *Vet Ophthalmol* 2015; 18(4):317–25. <https://doi.org/10.1111/vop.12241> PMID: [25495909](#)
13. Rama P, Matuska S, Paganoni G, Spinelli A, De Luca M, Pellegrini G. Limbal stem-cell therapy and long-term corneal regeneration. *N Engl J Med* 2010; 363(2):147–55. <https://doi.org/10.1056/NEJMoa0905955> PMID: [20573916](#)
14. Vlahović K. In vitro cultivation of canine limbal transplant. In: Pirkić B, Popović I, Borošak H, Hohšteter M, Kiš I, Matijatko V, Muljačić A, Špoljarić D, Popović M, editors: *Fakultet veterinarske medicine*.

15. Funderburgh JL, Mann MM, Funderburgh ML. Keratocyte phenotype mediates proteoglycan structure: a role for fibroblasts in corneal fibrosis. *J Biol Chem* 2003; 278(46):45629–37. <https://doi.org/10.1074/jbc.M303292200> PMID: 12933807
16. Villatoro AJ, Fernandez V, Claros S, Alcoholado C, Cifuentes M, Merayo-Llives J, et al. Regenerative Therapies in Dry Eye Disease: From Growth Factors to Cell Therapy. *Int J Mol Sci* 2017; 18(11). <https://doi.org/10.3390/ijms18112264> PMID: 29143779
17. Villatoro AJ, Claros S, Fernandez V, Alcoholado C, Farinas F, Moreno A, et al. Safety and efficacy of the mesenchymal stem cell in feline eosinophilic keratitis treatment. *BMC Vet Res* 2018; 14(1):116. <https://doi.org/10.1186/s12917-018-1413-4> PMID: 29587744
18. Villatoro AJ, Fernandez V, Claros S, Rico-Llanos GA, Becerra J, Andrades JA. Use of adipose-derived mesenchymal stem cells in keratoconjunctivitis sicca in a canine model. *Biomed Res Int* 2015; 2015:527926. <https://doi.org/10.1155/2015/527926> PMID: 25802852
19. Villatoro AJ, Alcoholado C, Martin-Astorga MC, Fernandez V, Cifuentes M, Becerra J. Comparative analysis and characterization of soluble factors and exosomes from cultured adipose tissue and bone marrow mesenchymal stem cells in canine species. *Vet Immunol Immunopathol* 2019; 208:6–15. <https://doi.org/10.1016/j.vetimm.2018.12.003> PMID: 30712794
20. Lotvall J, Hill AF, Hochberg F, Buzas EI, Di Vizio D, Gardiner C, et al. Minimal experimental requirements for definition of extracellular vesicles and their functions: a position statement from the International Society for Extracellular Vesicles. *J Extracell Vesicles* 2014; 3:26913. <https://doi.org/10.3402/jev.v3.26913> PMID: 25536934
21. Thoft RA, Friend J. The X, Y, Z hypothesis of corneal epithelial maintenance. *Invest Ophthalmol Vis Sci* 1983; 24(10):1442–3. PMID: 6618809
22. Nowell CS, Radtke F. Corneal epithelial stem cells and their niche at a glance. 2017.
23. Watt FM, Huck WT. Role of the extracellular matrix in regulating stem cell fate. *Nat Rev Mol Cell Biol* 2013; 14(8):467–73. <https://doi.org/10.1038/nrm3620> PMID: 23839578
24. Joe AW, Yeung SN. Concise review: identifying limbal stem cells: classical concepts and new challenges. *Stem Cells Transl Med* 2014; 3(3):318–22. <https://doi.org/10.5966/sctm.2013-0137> PMID: 24327757
25. Schlotzer-Schrehardt U, Kruse FE. Identification and characterization of limbal stem cells. *Exp Eye Res* 2005; 81(3):247–64. <https://doi.org/10.1016/j.exer.2005.02.016> PMID: 16051216
26. Maurer M, von Stebut E. Macrophage inflammatory protein-1. *Int J Biochem Cell Biol* 2004; 36(10):1882–6. <https://doi.org/10.1016/j.biocel.2003.10.019> PMID: 15203102
27. Russo RC, Garcia CC, Teixeira MM, Amaral FA. The CXCL8/IL-8 chemokine family and its receptors in inflammatory diseases. *Expert Rev Clin Immunol* 2014; 10(5):593–619. <https://doi.org/10.1586/1744666X.2014.894886> PMID: 24678812
28. Li J, Shen J, Beuerman RW. Expression of toll-like receptors in human limbal and conjunctival epithelial cells. *Mol Vis*. Volume 132007. p 813–22. PMID: 17615542
29. Ueta M, Hamuro J, Kiyono H, Kinoshita S. Triggering of TLR3 by poly(I:C) in human corneal epithelial cells to induce inflammatory cytokines. *Biochem Biophys Res Commun* 2005; 331(1):285–94. <https://doi.org/10.1016/j.bbrc.2005.02.196> PMID: 15845391
30. Gnecci M, Danielli P, Malpasso G, Ciuffreda M. Paracrine Mechanisms of Mesenchymal Stem Cells in Tissue Repair. In: Gnecci M, ed. *Methods in Molecular Biology*. 2nd ed. New York: Massimiliano Gnecci; 2016. p. 123–146.
31. Zhang J, Huang C, Feng Y, Li Y, Wang W. Comparison of beneficial factors for corneal wound-healing of rat mesenchymal stem cells and corneal limbal stem cells on the xenogeneic acellular corneal matrix in vitro. *Mol Vis* 2012; 18:161–73. PMID: 22275807
32. Kyurkchiev D, Bochev I, Ivanova-Todorova E, Mourdjeva M, Oreshkova T, Belemezova K, et al. Secretion of immunoregulatory cytokines by mesenchymal stem cells. *World J Stem Cells* 2014; 6(5):552–70. <https://doi.org/10.4252/wjsc.v6.i5.552> PMID: 25426252
33. Keino H, Horie S, Sugita S. Immune Privilege and Eye-Derived T-Regulatory Cells. *J Immunol Res* 2018; 2018. <https://doi.org/10.1155/2018/1679197> PMID: 29888291
34. Zhou R, Caspi RR. Ocular immune privilege. *F1000 Biol Rep*. Volume 22010. <https://doi.org/10.3410/B2-3> PMID: 20948803
35. Simpson RJ, Jensen SS, Lim JW. Proteomic profiling of exosomes: current perspectives. *Proteomics* 2008; 8(19):4083–99. <https://doi.org/10.1002/pmic.200800109> PMID: 18780348
36. Reiner AT, Witwer KW, van Balkom BWM, de Beer J, Brodie C, Corteling RL, et al. Concise Review: Developing Best-Practice Models for the Therapeutic Use of Extracellular Vesicles. *Stem Cells Transl Med* 2017; 6(8):1730–1739. <https://doi.org/10.1002/sctm.17-0055> PMID: 28714557

37. Han KY, Tran JA, Chang JH, Azar DT, Zieske JD. Potential role of corneal epithelial cell-derived exosomes in corneal wound healing and neovascularization. *Sci Rep* 2017; 7:40548. <https://doi.org/10.1038/srep40548> PMID: 28165027
38. Leszczynska A, Kulkarni M, Ljubimov AV, Saghizadeh M. Exosomes from normal and diabetic human corneolimbal keratocytes differentially regulate migration, proliferation and marker expression of limbal epithelial cells. *Sci Rep* 2018; 8(1):15173. <https://doi.org/10.1038/s41598-018-33169-5> PMID: 30310159
39. Samaeekia R, Rabiee B, Putra I, Shen X, Park YJ, Hematti P, et al. Effect of Human Corneal Mesenchymal Stromal Cell-derived Exosomes on Corneal Epithelial Wound Healing. *Invest Ophthalmol Vis Sci* 2018; 59(12):5194–200. <https://doi.org/10.1167/iovs.18-24803> PMID: 30372747
40. Wilson SE, Mohan RR, Ambrosio R Jr., Hong J, Lee J. The corneal wound healing response: cytokine-mediated interaction of the epithelium, stroma, and inflammatory cells. *Prog Retin Eye Res* 2001; 20(5):625–37. [https://doi.org/10.1016/s1350-9462\(01\)00008-8](https://doi.org/10.1016/s1350-9462(01)00008-8) PMID: 11470453
41. Ljubimov AV, Saghizadeh M. Progress in corneal wound healing. *Prog Retin Eye Res* 2015; 49:17–45. <https://doi.org/10.1016/j.preteyeres.2015.07.002> PMID: 26197361
42. Torricelli AA, Santhanam A, Wu J, Singh V, Wilson SE. The corneal fibrosis response to epithelial-stromal injury. *Exp Eye Res* 2016; 142:110–8. <https://doi.org/10.1016/j.exer.2014.09.012> PMID: 26675407
43. Wright B, Hopkinson A, Leyland M, Connon CJ. The secretome of alginate-encapsulated limbal epithelial stem cells modulates corneal epithelial cell proliferation. *PLoS One* 2013; 8(7):e70860. <https://doi.org/10.1371/journal.pone.0070860> PMID: 23894686
44. Shojaati G, Khandaker I, Funderburgh ML, Mann MM, Basu R, Stolz DB, et al. Mesenchymal Stem Cells Reduce Corneal Fibrosis and Inflammation via Extracellular Vesicle-Mediated Delivery of miRNA. *Stem Cells Transl Med* 2019; 8(11):1192–1201. <https://doi.org/10.1002/sctm.18-0297> PMID: 31290598
45. Majo F, Rochat A, Nicolas M, Jaoude GA, Barrandon Y. Oligopotent stem cells are distributed throughout the mammalian ocular surface. *Nature* 2008; 456(7219):250–4. <https://doi.org/10.1038/nature07406> PMID: 18830243
46. Kafarnik C, McClellan A, Dziasko M, Daniels JT, Guest DJ. Canine Corneal Stromal Cells Have Multipotent Mesenchymal Stromal Cell Properties In Vitro. *Stem Cells Dev* 2020. <https://doi.org/10.1089/scd.2019.0163> PMID: 31973649